Title

Development of a Comprehensive Osteochondral Allograft MRI Scoring System (OCAMRISS) With Histopathologic, Micro–Computed Tomography, and Biomechanical Validation

Journal

Cartilage, 5(1)

ISSN

1947-6035

Authors

Chang, Eric Y

Pallante-Kichura, Andrea L

Bae, Won C

et al.

Publication Date

2014

DOI

10.1177/1947603513514436

Peer reviewed

Cartilage
2014, Vol 5(1) 16–27

DOI: 10.1177/1947603513514436
cart.sagepub.com
SAGE

Development of a Comprehensive Osteochondral Allograft MRI Scoring System (OCAMRISS) With Histopathologic, Micro–Computed Tomography, and Biomechanical Validation

Eric Y. Chang[1,2], Andrea L. Pallante-Kichura[3], Won C. Bae[2], Jiang Du[2], Sheronda Statum[2], Tanya Wolfson[2], Anthony C. Gamst[2], Esther Cory[3], David Amiel[4], William D. Bugbee[4,5], Robert L. Sah[3,4], and Christine B. Chung[1,2]

Abstract

Objective: To describe and apply a semiquantitative MRI scoring system for multifeature analysis of cartilage defect repair in the knee by osteochondral allografts and to correlate this scoring system with histopathologic, micro–computed tomography (μCT), and biomechanical reference standards using a goat repair model. *Design*: Fourteen adult goats had 2 osteochondral allografts implanted into each knee: one in the medial femoral condyle and one in the lateral trochlea. At 12 months, goats were euthanized and MRI was performed. Two blinded radiologists independently rated 9 primary features for each graft, including cartilage signal, fill, edge integration, surface congruity, calcified cartilage integrity, subchondral bone plate congruity, subchondral bone marrow signal, osseous integration, and presence of cystic changes. Four ancillary features of the joint were also evaluated, including opposing cartilage, meniscal tears, synovitis, and fat-pad scarring. Comparison was made with histologic and μCT reference standards as well as biomechanical measures. Interobserver agreement and agreement with reference standards was assessed. Cohen's κ, Spearman's correlation, and Kruskal-Wallis tests were used as appropriate. *Results*: There was substantial agreement ($\kappa > 0.6$, $P < 0.001$) for each MRI feature and with comparison against reference standards, except for cartilage edge integration ($\kappa = 0.6$). There was a strong positive correlation between MRI and reference standard scores ($\rho = 0.86$, $P < 0.01$). Osteochondral allograft MRI scoring system was sensitive to differences in outcomes between the types of allografts. *Conclusions*: We have described a comprehensive MRI scoring system for osteochondral allografts and have validated this scoring system with histopathologic and μCT reference standards as well as biomechanical indentation testing.

Keywords

cartilage repair, osteochondral allografts, MRI scoring system

Introduction

Localized articular cartilage lesions in young patients are relatively common,[1] and treatment remains a challenge. A number of repair strategies exist, including microfracture, osteochondral autograft transfer, and cell-based transplantation techniques, but each has its own limitations.[2-8] Osteochondral allograft transplantation is an attractive technique that allows for the simultaneous resurfacing of large articular defects and the correction of underlying bone abnormalities. In some ways, osteochondral allografts are ideal for transplantation because cartilage is a relatively immunoprivileged tissue,[9] mature living chondrocytes can survive for many years after transplantation without tissue matching or immunosuppression,[10] and bone has the potential to heal and remodel.[11-13]

There have been a number of histopathologic,[14] surgical,[15,16] and imaging-based,[17-22] cartilage repair scoring systems developed to address the need for objective and

[1]Department of Radiology, VA San Diego Healthcare System, San Diego, CA, USA
[2]Department of Radiology, University of California, San Diego Medical Center, La Jolla, CA, USA
[3]Department of Bioengineering, University of California, San Diego, CA, USA
[4]Department of Orthopaedic Surgery, University of California, San Diego School of Medicine, La Jolla, CA, USA
[5]Department of Orthopaedic Surgery, Scripps Clinic, La Jolla, CA, USA

Corresponding Author:
Eric Y. Chang, San Diego Healthcare System, 3350 La Jolla Village Drive, MC 114, San Diego, CA 92161, USA.
Email: ericchangmd@gmail.com

Table 1. Imaging Parameters.

Sequence	Plane	TR (ms)	TI (ms)	TE (ms)	Matrix	Thickness (mm)	FOV (cm)	Voxel Size (μm^3)	Projections	Flip Angle (°)	Bandwidth (Hz)/Pixel	ETL	NEX
Intermediate-weighted	Sag	3,600	—	32	384 × 384	1.7	10	260 × 260 × 1700	—	90	122.1	7	1
Intermediate-weighted	Cor	3,600	—	32	384 × 384	1.7	10	260 × 260 × 1700	—	90	122.1	7	1
Intermediate-weighted	Ax	3,600	—	32	384 × 384	1.7	10	260 × 260 × 1700	—	90	122.1	7	1
STIR	Sag	3,000	170	17	320 × 192	1.7	10	313 × 521 × 1700	—	90	146.3	2	1
STIR	Ax	3,000	170	17	320 × 192	1.7	10	313 × 521 × 1700	—	90	146.3	2	1
PD-weighted	Sag	3,200	—	8	320 × 256	1.7	10	313 × 391 × 1700	—	90	162.5	1	1
PD-weighted	Ax	3,200	—	8	320 × 256	1.7	10	313 × 391 × 1700	—	90	162.5	1	1
T1-weighted	Sag	700	—	11	384 × 384	1.7	10	260 × 260 × 1700	—	90	122.1	5	1
2D UTE, multi-echo, with fat-saturation	Sag	475	—	0.012 and 4	384 × 384	1.7	10	260 × 260 × 1700	455	45	325.5	—	2
3D UTE, multi-echo, with fat-saturation	Sag	22	—	0.012 and 4	384 × 384	0.31	12	260 × 260 × 260	44,000	14	325.5	—	1

TR = repetition time; TI = inversion time; TE = echo time; FOV = field of view; ETL = echo train length; NEX = number of excitations; STIR = short TI inversion recovery; PD = proton density; UTE = ultrashort echo time; Sag = sagittal; Cor = coronal; Ax = axial.

reliable comparison between different therapeutic approaches. Unlike histopathologic[23,24] and surgical scoring systems,[25,26] however, there are a paucity of studies which have validated MRI scoring systems. Recent studies have shown a lack of strong evidence for MRI to predict clinical outcome,[27] including with the widely used Magnetic Resonance Observation of Cartilage Repair Tissue (MOCART) score.[28] Validation of the individual components of a noninvasive scoring system is a logical first step to understanding this discord.

We have used and evaluated a number of osteochondral allografts in our practice and have recognized the need for accurate noninvasive characterization. Furthermore, while imaging grading systems that are used to compare *between* various cartilage repair techniques are useful, we have found that they may not be optimized for comparing features *unique* to a certain technique. For instance, grading systems that are optimized to address cartilage defect repair with cell-based transplantation techniques (such as the MOCART score) are not optimal to evaluate techniques that involve osteochondral transfer *en bloc*. This is further highlighted with the introduction of the 3D MOCART score, which includes "bone interface," which describes integration of the transplant to the native subchondral bone as well as integration of a possible periosteal flap and "chondral osteophytes," which are a complication described with cartilage transplantation and bone marrow stimulating techniques.[29] Additionally, to our knowledge, there are no studies that systematically compare a comprehensive grading system with reference standard validation. In part this is because of the fact that most means for validation are invasive, including second look arthroscopy and biopsy. Animal models are useful to circumvent these limitations.

The purpose of this study was to (1) describe and apply a semiquantitative MRI scoring system for multifeature analysis of cartilage defect repair by osteochondral allografts and (2) to correlate this scoring system with histopathologic, micro–computed tomography (μCT), and biomechanical reference standards using a goat repair model.

Methods

Tissues analyzed were from a previously published study in an adult Boer goat model.[30] Although the previous study used 15 goats,[30] only 14 were imaged and included in this study. All experiments were carried out in accordance with protocols approved by the Institutional Animal Care and Use Committee. In brief, each goat was operated in one knee and each knee received 2 orthotopic osteochondral allografts measuring 8 × 5 mm (diameter × depth). Grafts were implanted into 7.5 × 5 mm (diameter × depth) defects in the medial femoral condyle (MFC) and lateral trochlea (LT). Four different groups of graft storage were analyzed, including fresh (n = 7), 14-day storage at 4 °C (n = 7), 28-day storage at 4 °C (n = 7), and frozen grafts (n = 7). At 12 months, goats were euthanized and MRI was performed and compared with histopathologic, μCT, and biomechanical analysis.

MRI Technique

Imaging was performed on a 3T clinical MRI scanner (Signa Twinspeed, GE Healthcare, Milwaukee, WI) with a wrist coil. Hardware modification included an addition of a custom transmit–receive switch to the receiver preamplifiers for rapid switching after the end of a radiofrequency excitation pulse, which allows for detection of signal as early as 8 μs. Imaging parameters are listed in **Table 1**. In brief, 2D imaging sequences consisted of 3-plane intermediate-weighted fast spin echo (FSE) sequences, sagittal and axial

STIR and proton density–weighted conventional spin echo sequences, and sagittal T1-weighted FSE sequences. Additionally, sagittal 2D and 3D multi-echo ultrashort echo time (UTE) sequences with fat saturation were obtained with subtraction of the second echo from the first to generate images that highlight short T2* tissues.[31,32] However, for this study, the whole UTE data set was not used, but rather only the subtraction images for evaluation of the deep cartilage of the graft (feature 5, see below). Although the 3D UTE source images are higher in spatial resolution and sensitive to both long and short T2* tissues, we felt there may have been limited translatability had we used the source images for comprehensive MRI feature analysis since not all investigators have access to this particular sequence. Therefore, the MRI readers were blinded to the UTE source images.

Our imaging resolution parameters were modified from our typical clinical knee examination to account for the relatively smaller dimensions of the goat knee. Specifically, we calculated that volumes of goat distal femoral epiphyses used in our study were approximately 24% of the volume of human distal femoral epiphyses. Therefore, voxels used in this study were scaled to 24% of that used in our clinical knee protocols.

MRI Analysis

Images were evaluated independently by 2 blinded fellowship-trained musculoskeletal radiologists (reader A [EYC] and reader B [CBC], with 2 and 15 years of experience, respectively). Based on our experience with osteochondral allografts, we have created the semiquantitative *O*steo*C*hondral *A*llograft *MRI S*coring *S*ystem (OCAMRISS), which includes 9 *primary* features of the graft (5 cartilage and 4 bone) and 4 *ancillary* features of the joint, as shown in **Table 2**. Each MRI-determined *primary* feature also had a corresponding reference standard, determined either histopathologically or on μCT.[30] Specifically, *primary* features for *cartilage* included (1) cartilage signal of the graft relative to adjacent host cartilage, (2) cartilage "fill" of the graft (percentage volume), (3) cartilage edge integration at the host-graft junction, (4) cartilage surface congruity of the graft and host-graft junction, (5) calcified cartilage integrity of the graft, and for *bone* included (6) subchondral bone plate congruity of the graft and host-graft junction, (7) subchondral bone marrow signal intensity of the graft relative to epiphyseal bone, (8) osseous integration at the host-graft junction, and (9) presence of cystic changes of the graft and host-graft junction. *Ancillary* features of the joint were evaluated using similar criteria as in multiple prior studies and included detecting abnormalities of (10) opposing medial tibial plateau cartilage,[33] (11) meniscal tears,[34,35] (12) synovitis,[36,37] and (13) infrapatellar fat pad scarring.[37,38]

Corresponding Reference Standards

As part of a prior study,[30] μCT, histopathology, and biomechanical indentation testing was performed on retrieved tissue after euthanization. The MRI results were compared with modified Mankin (MM) scores[39] from that study. In brief, sagittal slices through the central portion of the grafts were prepared and stained at 7 μm thickness and the MM score was used to assess the graft cartilage with a minimum score of 0, representing normal cartilage, and a maximum score of 15, representing the highest degree of degeneration. The MRI results were also compared with cartilage loadbearing function data from that prior study.[30] In brief, indentation testing was performed at the center of each graft and stiffness was calculated (expressed in units of MPa).

For the current study, a blinded reviewer (ALP) evaluated the μCT images for (1) subchondral bone plate integrity and congruity, (2) osseous integration, and (3) presence of intraosseous cystic changes. (1) Subchondral bone plate was scored as intact within the graft and flush at host-graft junction (score 0) or disrupted within the graft or offset greater than one subchondral bone plate thickness (score 1). (2) Osseous integration at the host-graft junction was scored as normal if trabeculae crossed the circumferential interface (score 0) or abnormal if there was a region without crossing trabeculae (score 1). (3) Intraosseous cystic changes within the graft or at the host-graft junction, defined as trabeculae voids with a maximum diameter of greater than 2.0 mm, were scored as absence of cystic changes (score 0) or presence of cystic changes (score 1).

A blinded reviewer (ALP) also scored the hematoxylin and eosin (H&E) slides for degree of cartilage filling, similar to the corresponding MRI variable where cartilage "fill" of the graft (percentage volume) was scored as 76% to 100% (score 0), 51% to 75%, greater than 100% (score 1), and less than 50% (score 2). Cartilage edge integration at host-graft junction was scored as no discernible fissure (score 0), discernible fissure (score 1), and fissure >1 mm (score 2). The cartilage surface congruity of the graft and host was evaluated and designated as entirely flush (score 0), less than 50% offset compared with host cartilage thickness (score 1), or greater than 50% offset compared with the host cartilage thickness (score 2). Calcified cartilage integrity was designated as present and intact (score 0) or thinned/absent (score 1). Subchondral bone was designated as normal (score 0) or abnormal (score 1) if there were histologic features typically associated with bone marrow edema pattern lesions, including swollen fat cells surrounded by eosinophilic staining, fibrous tissue, or increased trabeculae.[40,41]

Statistical Analysis

Statistical analyses were performed with R (v2.15, 2012, R Foundation for Statistical Computing, Vienna, Austria).

Table 2. Grading Scheme.

MRI Feature	MRI Score	Reference Standard	Reference Standard Score
1. Cartilage signal of graft	0: Normal 1: Altered intensity (either hypointense or hyperintense, but not fluid) 2: Fluid signal intensity on all sequences	Histopathology	Modified Mankin (0-15)
2. Cartilage "fill" of graft (percentage of volume)	0: 76% to 100% 1: 51% to 75% or >100% 2: <50%	Histopathology	0: 76% to 100% 1: 51% to 75% or >100% 2: <50%
3. Cartilage edge integration at host-graft junction	0: No discernible boundary 1: Discernible boundary 2: Discernible fissure >1 mm	Histopathology	0: No discernible fissure 1: Discernible fissure 2: Discernible fissure >1 mm
4. Cartilage surface congruity of graft and host-graft junction	0: Flush 1: <50% offset of host cartilage 2: >50% offset of host cartilage	Histopathology	0: Flush 1: <50% offset 2: >50% offset
5. Calcified cartilage integrity of graft	0: Intact, thin, and smooth 1: Altered (disrupted, thickened, or blurred)	Histopathology	0: Present and intact 1: Thinned or absent
6. Subchondral bone plate congruity of graft and host-graft junction	0: Intact and flush 1: Disrupted or not flush by >1 subchondral thickness	μCT	0: Intact and flush 1: Disrupted or offset by >1 subchondral thickness
7. Subchondral bone marrow signal intensity of graft relative to epiphyseal bone	0: Normal 1: Abnormal (bone marrow edema pattern or hypointensity on all sequences)	Histopathology	0: <33% area with swollen fat cells, fibrous tissue, or increased trabeculae 1: >33% abnormal area
8. Osseous integration at host-graft junction	0: Crossing trabeculae 1: Discernible cleft	μCT	0: Circumferentially crossing trabeculae 1: Region without crossing trabeculae
9. Presence of cystic changes of graft and host-graft junction	0: Absent 1: Present	μCT	0: Absent 1: Cyst >1.0 mm present
10. Opposing cartilage	0: Normal 1: Abnormal	N/A	N/A
11. Meniscal tears	0: Absent 1: Present		
12. Synovitis			
13. Fat pad scarring			

Table includes 9 *primary* features with reference standard validation (5 cartilage [features 1-5] and 4 bone [features 6-9]) and 4 *ancillary* features of the joint (features 10-13) without reference standard validation.

Unweighted κ was used to assess interobserver agreement for individual MRI features. Features 1 to 13 were added together and designated as a 13-feature Total Score for MRI (TS13-MRI). Intraclass correlation coefficient (ICC) was used to assess interobserver agreement for TS13-MRI.

Unweighted κ was used to assess agreement between individual MRI features and reference standards where available and the two kappa values (one for each reader) were averaged in order to maintain the same scale as the reference standard. For the remainder of analyses, MRI scores of the 2 readers were averaged and the average was used. Spearman's correlation was used to examine the ordinal relationship for feature 1 MRI score (cartilage signal) versus MM score. Features 1 to 9 were added together and designated as a 9-feature Total Score for MRI (TS9-MRI) values and as a 9-feature Total Score for reference standard (TS9-REF) values based on histopathology and μCT. Spearman's correlation was used to evaluate the relationship between TS9-MRI and TS9-REF.

Spearman's correlation was also used to assess the relationship between TS13-MRI scores and indentation stiffness for MFC and LT grafts both as a group and separately. Kruskal-Wallis test was performed to detect significant differences between groups based on type of graft storage for TS9-MRI

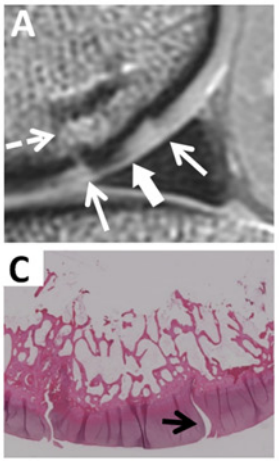

E Feature	OCAMRISS (Figures A and B)	Reference Score (Figures C and D)
1. Cartilage signal of graft	0 (thick arrow)	Mod. Mankin = 1
2. Cartilage "fill" of graft	0 (thick arrow)	0
3. Cartilage edge integration	1 (thin arrows)	1
4. Cartilage surface congruity	0 (thin arrows)	0 (black arrow)
5. Calcified cartilage integrity	0 (curved arrow)	0
6. Subchondral bone plate congruity	1	1 (arrowhead)
7. Subchondral bone marrow signal	0 (dashed arrow)	0
8. Osseous integration	0 (dashed arrow)	0
9. Presence of cystic changes	1 (not shown)	1 (not shown)
TOTAL	3	4

Figure 1. Medial femoral condyle allograft with fresh storage and good performance (OCAMRISS TS9-MRI 3 points and TS9-REF 4 points; cartilage stiffness = 4.2 MPa). Sagittal proton density (PD)–weighted image (**A**), sagittal 3D ultrashort echo time (UTE) subtraction image (**B**), hematoxylin and eosin stain (**C**), and micro–computed tomography (**D**) demonstrate features as listed in the accompanying table (**E**).

and TS9-REF scores. To adjust for within-knee dependence, bootstrap-based techniques were used to compute 95% confidence intervals (CI) for the ICCs and correlation coefficients, and to assess p-values as appropriate. Kappa statistics were interpreted as 0 to 0.2, slight; 0.21 to 0.4, fair; 0.41 to 0.6, moderate; 0.61 to 0.80, substantial; 0.81 to 1.0, almost perfect.[42]

Despite being underpowered for a subanalysis (and not likely to detect results), a purely exploratory subanalysis was performed to determine which individual features of OCAMRISS would best predict biomechanical indentation stiffness. Each individual OCAMRISS feature was used as a predictor in a mixed-effects regression with stiffness as outcome, covarying for type of storage and with a subject-specific intercept fitted. The averages of both readers were used for each OCAMRISS MRI feature.

Results

The OCAMRISS method was successfully applied to a data set designed to have variable treatment outcome, ranging from outstanding to poor (**Figs. 1-4**).

Interobserver Agreement

There was substantial to almost perfect agreement for all MRI score components ($\kappa > 0.7$, $P < 0.001$; **Table 3**). Although there was perfect interobserver agreement for feature 8 (osseous integration), κ could be not be calculated because of lack of variability since both readers scored all 28 grafts the same (score 0, evidence for crossing trabeculae). Reader agreement was excellent for TS13-MRI (ICC = 0.982, CI = [0.965, 0.992]).

MRI Scores Compared With Reference Standards

For feature 1 (cartilage signal), there was only one disagreement between the 2 readers and there was a strong positive correlation of the MRI scores with MM score ($\rho = 0.68$, $P < 0.0001$). Agreement of MRI score for feature 3 (cartilage edge integration) compared with the reference standard was moderate ($\kappa = 0.6$). For all other features, there was substantial to almost perfect agreement between MRI and reference standard scores ($\kappa > 0.6$, $P < 0.0001$). Again, κ could not be calculated for feature 8, but there was perfect agreement. **Figure 5** shows the relationship between TS9-MRI versus TS9-REF ($\rho = 0.855$, CI = [0.708, 0.928]).

Correlation between TS13-MRI with indentation stiffness was significantly negative ($\rho = -0.528$, CI = [−0.746, −0.149]) and this relationship strengthened when evaluating for only MFC grafts ($\rho = -0.788$, CI = [−0.948, -−0.374]), in part due to a wider range of LT graft stiffness (**Fig. 6**). The Kruskal-Wallis test detected significant differences between storage subgroups of TS9-MRI and TS9-REF with the frozen group performing worse than the other 3 groups ($P = 0.007$ and $P = 0.001$, respectively; **Fig. 7**).

The purely exploratory subanalysis was performed on all OCAMRISS features except feature 8 where there was no variability. The mixed-effects regression showed that the only observed difference was in feature 5, with higher stiffness when the calcified cartilage was normal on UTE subtraction images ($P = 0.0239$). As this was an exploratory subanalysis, results from this mixed-effects regression require validation with independent data.

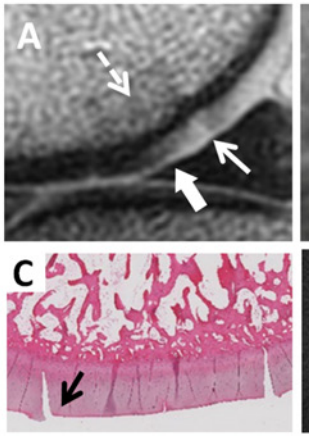

E Feature	OCAMRISS (Figures A and B)	Reference Score (Figures C and D)
1. Cartilage signal of graft	0 (thick arrow)	Mod. Mankin = 6
2. Cartilage "fill" of graft	0 (thick arrow)	0
3. Cartilage edge integration	1 (thin arrow)	1
4. Cartilage surface congruity	0 (thin arrow)	0 (black arrow)
5. Calcified cartilage integrity	0 (curved arrow)	0
6. Subchondral bone plate congruity	0	0 (arrowhead)
7. Subchondral bone marrow signal	0 (dashed arrow)	0
8. Osseous integration	0 (dashed arrow)	0 (boxed arrow)
9. Presence of cystic changes	0	0
TOTAL	1	7

Figure 2. Medial femoral condyle allograft stored at 4 °C × 14 days with outstanding performance (OCAMRISS TS9-MRI 1 point and TS9-REF 7 points; cartilage stiffness = 5.1 MPa). Sagittal proton density (PD)–weighted image (**A**), sagittal 3D ultrashort echo time (UTE) subtraction image (**B**), hematoxylin and eosin stain (**C**), and micro–computed tomography (**D**) demonstrate features as listed in the accompanying table (**E**).

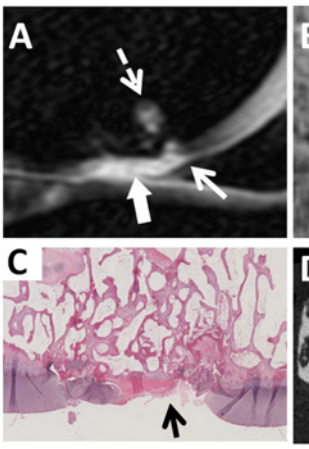

E Feature	OCAMRISS (Figures A and B)	Reference Score (Figures C and D)
1. Cartilage signal of graft	2 (thick arrow)	Mod. Mankin = 15
2. Cartilage "fill" of graft	2 (thick arrow)	2 (black arrow)
3. Cartilage edge integration	2 (thin arrow)	2
4. Cartilage surface congruity	2	2
5. Calcified cartilage integrity	1 (curved arrow)	1
6. Subchondral bone plate congruity	1	1 (arrowhead)
7. Subchondral bone marrow signal	1	1
8. Osseous integration	0	0
9. Presence of cystic changes	1 (dashed arrow)	1 (dashed arrow)
TOTAL	12	25

Figure 3. Medial femoral condyle allograft with frozen storage and poor performance (OCAMRISS TS9-MRI 12 points and TS9-REF 25 points; cartilage stiffness = 0.2 MPa). Sagittal short TI inversion recovery (STIR) image (**A**), sagittal 3D ultrashort echo time (UTE) subtraction image (**B**), hematoxylin and eosin stain (**C**), and micro–computed tomography (**D**) demonstrate features as listed in the accompanying table (**E**).

Discussion

In this study, we have described a comprehensive, semi-quantitative MRI scoring system for analysis of cartilage defect repair by osteochondral allografts, which we have termed OCAMRISS (*O*steo*C*hondral *A*llograft *MRI S*coring *S*ystem). The OCAMRISS method shows substantial interobserver agreement, substantial agreement with histopathologic and μCT reference standards for nearly all primary features, and significant negative correlation with biomechanical indentation testing. It is known from multiple prior reports that fresh and refrigerated osteochondral allografts perform better than frozen allografts,[30,43-46] likely because of differences in cell viability, and OCAMRISS was sensitive to the differences in outcomes between these groups.

The OCAMRISS method was designed and validated on osteochondral allografts. However, where appropriate, we incorporated features from one of the most widely used MRI scoring systems after cartilage repair, the MOCART score.[28] The MOCART score includes 9 variables: the degree of filling of the defect, integration to the border

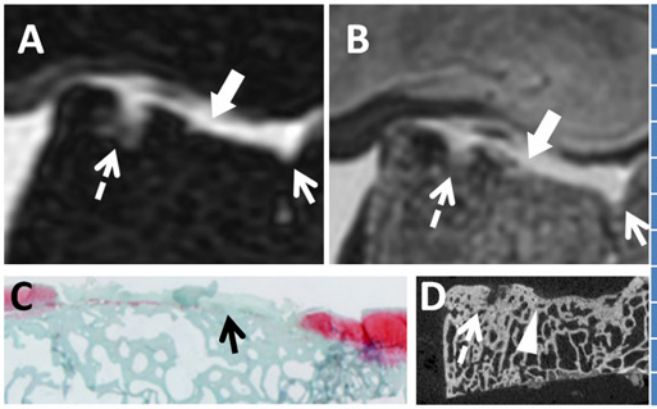

E Feature	OCAMRISS (Figures A and B)	Reference Score (Figures C and D)
1. Cartilage signal of graft	2 (thick arrow)	Mod. Mankin = 13
2. Cartilage "fill" of graft	2 (thick arrow)	2 (black arrow)
3. Cartilage edge integration	2 (thin arrow)	2
4. Cartilage surface congruity	2	2
5. Calcified cartilage integrity	1	1
6. Subchondral bone plate congruity	1	1 (arrowhead)
7. Subchondral bone marrow signal	1	1
8. Osseous integration	0	0
9. Presence of cystic changes	1 (dashed arrow)	1 (dashed arrow)
TOTAL	**12**	**23**

Figure 4. Lateral trochlea allograft with frozen storage and poor performance (OCAMRISS TS9-MRI 12 points and TS9-REF 23 points; cartilage stiffness, 0.1 MPa). Axial short TI inversion recovery (STIR) image (**A**), axial proton density (PD)–weighted image (**B**), Safranin-O stain (**C**), and micro–computed tomography (D) demonstrate features as listed in the accompanying table (**E**).

Table 3. Results of Interobserver Agreement and Agreement With Reference Standards.

Feature	Reader 1 Scores, Score (Number of Samples, %)	Reader 2 Scores, Score (Number of Samples, %)	Interobserver Agreement	Reference Standard Scores, Score (Number of Samples, %)	Agreement With Reference Standard (Reader A)	Agreement With Reference Standard (Reader B)	Average κ for Readers A and B
1. Cartilage signal of graft	0 (14, 50%) 1 (10, 36%) 2 (4, 14%)	0 (14, 50%) 1 (9, 32%) 2 (5, 18%)	0.94	Mean modified Mankin 7.2 (SD 3.9, range 1-15)	N/A[a]	N/A[a]	N/A[a]
2. Cartilage "fill" of graft (percentage of volume)	0 (17, 61%) 1 (4, 14%) 2 (7, 25%)	0 (18, 64%) 1 (3, 11%) 2 (7, 25%)	0.93	0 (18, 64%) 1 (3, 11%) 2 (7, 25%)	0.93	1	0.97
3. Cartilage edge integration at host-graft junction	0 (4, 14%) 1 (20, 71%) 2 (4, 14%)	0 (3, 11%) 1 (18, 64%) 2 (7, 25%)	0.71	0 (3, 11%) 1 (21, 75%) 2 (4, 14%)	0.58	0.62	0.6
4. Cartilage surface congruity of graft and host-graft junction	0 (12, 43%) 1 (12, 43%) 2 (4, 14%)	0 (12, 43%) 1 (13, 46%) 2 (3, 11%)	0.94	0 (11, 39%) 1 (14, 50%) 2 (3, 11%)	0.88	0.94	0.91
5. Calcified cartilage integrity of graft	0 (11, 39%) 1 (17, 61%)	0 (13, 46%) 1 (15, 54%)	0.86	0 (13, 46%) 1 (15, 54%)	0.71	0.86	0.79
6. Subchondral bone plate congruity of graft and host-graft junction	0 (13, 46%) 1 (15, 54%)	0 (14, 50%) 1 (14, 50%)	0.93	0 (13, 46%) 1 (15, 54%)	1.00	0.93	0.96
7. Subchondral bone marrow signal intensity of graft relative to epiphyseal bone	0 (15, 54%) 1 (13, 46%)	0 (14, 50%) 1 (14, 50%)	0.93	0 (18, 64%) 1 (10, 36%)	0.64	0.57	0.61
8. Osseous integration at host-graft junction	0 (28, 100%) 1 (0, 0%)	0 (28, 100%) 1 (0, 0%)	Perfect agreement[b]	0 (28, 100%) 1 (0, 0%)	Perfect agreement[b]	Perfect agreement[b]	Perfect agreement[b]
9. Presence of cystic changes of graft and host-graft junction	0 (7, 25%) 1 (21, 75%)	0 (9, 32%) 1 (19, 68%)	0.83	0 (7, 25%) 1 (21, 75%)	1.00	0.83	0.91
10. Opposing cartilage	0 (20, 71%) 1 (8, 29%)	0 (20, 71%) 1 (8, 29%)	1		N/A[c]	N/A[c]	N/A[c]
11. Meniscal tears	0 (20, 71%) 1 (8, 29%)	0 (20, 71%) 1 (8, 29%)	1		N/A[c]	N/A[c]	N/A[c]
12. Synovitis	0 (26, 93%) 1 (2, 7%)	0 (26, 93%) 1 (2, 7%)	1		N/A[c]	N/A[c]	N/A[c]
13. Fat pad scarring	0 (26, 93%) 1 (2, 7%)	0 (26, 93%) 1 (2, 7%)	1		N/A[c]	N/A[c]	N/A[c]

[a]Spearman's correlation was used instead (refer to text).
[b]Kappa could not be calculated because of lack of variability (refer to text).
[c]Reference standards for features 10 to 13 were not available.

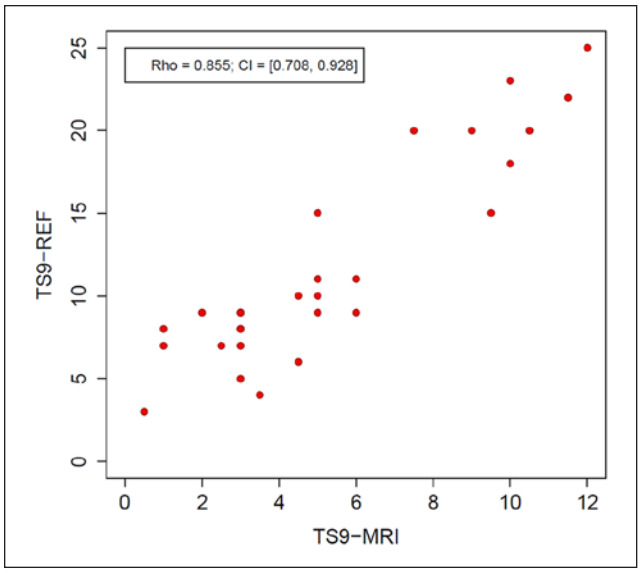

Figure 5. Graph of relationship between 9-feature MRI score (TS9-MRI) versus 9-feature reference standard score (TS9-REF). Spearman's ρ = 0.855, confidence interval [CI] = [0.708, 0.928].

zone, description of the surface, description of the structure, signal intensity, status of the subchondral lamina, status of the subchondral bone, appearance of adhesions, and presence of synovitis. Although some components of the MOCART score have been validated with certain repair techniques, such as surgical evaluation of the surface after microfracture[47] and autologous chondrocyte implantation,[48] to our knowledge, there are no prior studies that have systematically compared the constituents of an MRI grading system with reference standard validation.

There are many notable differences between OCAMRISS and the MOCART score (**Table 4**). The MOCART score only includes 2 variables for the evaluation of bone. MOCART score feature 6 (subchondral lamina) evaluates the subchondral bone plate beneath the repair tissue, and similar to prior authors[49] we have found the original description of this feature[28] to be ambiguous when applied to osteochondral grafts. Tetta et al[49] excluded this parameter when using the MOCART score on osteochondral grafts; however, we feel the evaluation of subchondral bone plate congruity, both of the graft and at the host-graft junction, is important and have included this into our system. MOCART feature 7 (subchondral bone) combines the evaluation for bone marrow edema lesions and cysts, whereas our system separates these features because of their histologic[40,41] and potential prognostic[50,51] differences. With regard to evaluation of cartilage, MOCART score feature 4 (structure of repair tissue) may be better suited for cell-based repair techniques, and corresponds to a combination of features 1 (cartilage signal intensity) and 2 (cartilage "fill") in our system. Additionally, despite oversizing the graft relative to the defect for a snug fit, cartilage of osteochondral grafts is unable to regenerate across a physical gap,[18,52-54] unlike cell-based repair techniques.[55] For this reason, none of our samples demonstrated complete chondral integration on histology. Therefore, delineation of "integration to the border zone" (MOCART score feature 2 and corresponding feature 3 of our grading scheme) should be made with this in mind since the best possible MRI outcome (score 0, no discernible boundary) will show a boundary at histology. We also did not include MOCART score feature 8 (presence of adhesions) into our classification since it may be more important in cell-based repair techniques, where it can lead to the requirement for arthroscopic debridement in up to 5% to 10% of patients.[28] Finally, evaluation of the calcified cartilage layer (feature 5) is unique to our system and made possible with the advent of UTE sequences.[56,57] The calcified cartilage layer is metabolically active,[58] remodels with changing loads,[59-61] and plays an important role in overall function of the osteochondral unit.[62]

In addition to the widely popular MOCART score, other authors have used various MRI scoring systems to characterize osteochondral grafts, but to our knowledge, no formal one-to-one comparison between scoring system components and corresponding reference standards has been made. Rather, prior studies have focused on the comparison between MRI and clinical outcomes,[17,19,20,22] histologic cellular viability,[17,18] histologic composition,[18] or immunologic responses.[21] Furthermore, both the OCAMRISS and the MOCART systems are more comprehensive in comparison with these prior studies.

Correlation between OCAMRISS and indentation stiffness was significantly negative, however the relationship strengthened when evaluating for only MFC grafts. This may have been because of several reasons. As we have previously noted, our sample demonstrated greater histopathologic and biomechanical variability at the LT compared with the MFC sites.[30] This is consistent with several clinical studies which have shown worse outcomes at patellofemoral lesions.[63-66] In addition to this, both MRI readers subjectively felt the MFC grafts were easier to score, in part due to increased volume averaging at the LT due to curvature of cartilage and because LT grafts were on average ~40% thinner (LT 0.72 ± 0.21 mm versus MFC 1.78 ± 0.54 mm).[30] For this reason, typically two planes were required for LT graft evaluation whereas a single plane was sufficient for MFC grafts. Despite these differences, a post hoc analysis determined that there was no detectable adverse effect of cartilage thickness on interobserver agreement or correlations used in this study. Additionally, our purely exploratory subanalysis suggests that calcified cartilage integrity (feature 5) as seen on UTE subtraction images may be particularly useful to predict biomechanical outcome. We are hopeful that OCAMRISS may serve as a springboard for future studies to independently validate this finding.

Our study has a number of limitations. First, our sample size was small. However, our main goal was to correlate

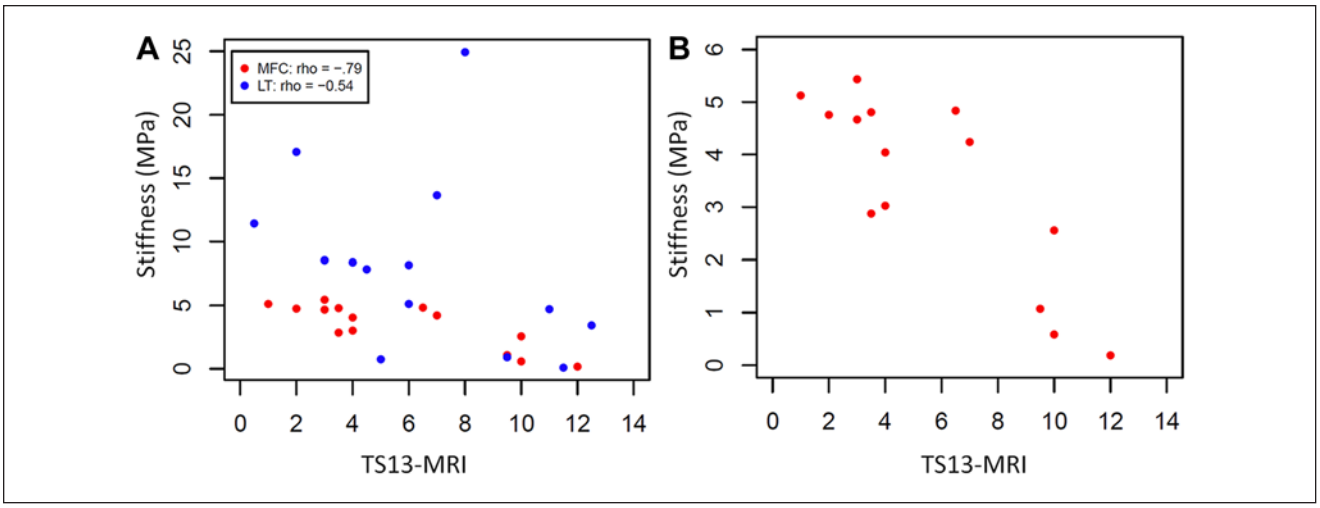

Figure 6. Graphs of 13-feature MRI score (TS13-MRI) versus biomechanical indentation stiffness for both medial femoral condyle (MFC) and lateral trochlea (LT) grafts (**A**) and only for MFC grafts (**B**). Spearman's ρ for combined MFC and LT grafts was significantly negative (ρ = −0.528, confidence interval [CI] = [−0.746, −0.149]) and the relationship strengthened when evaluating for only MFC grafts (ρ = −0.788, CI = [−0.948, −0.374]) as there was a wider range of stiffness for LT grafts. Red dots represent MFC grafts and blue dots represent LT grafts.

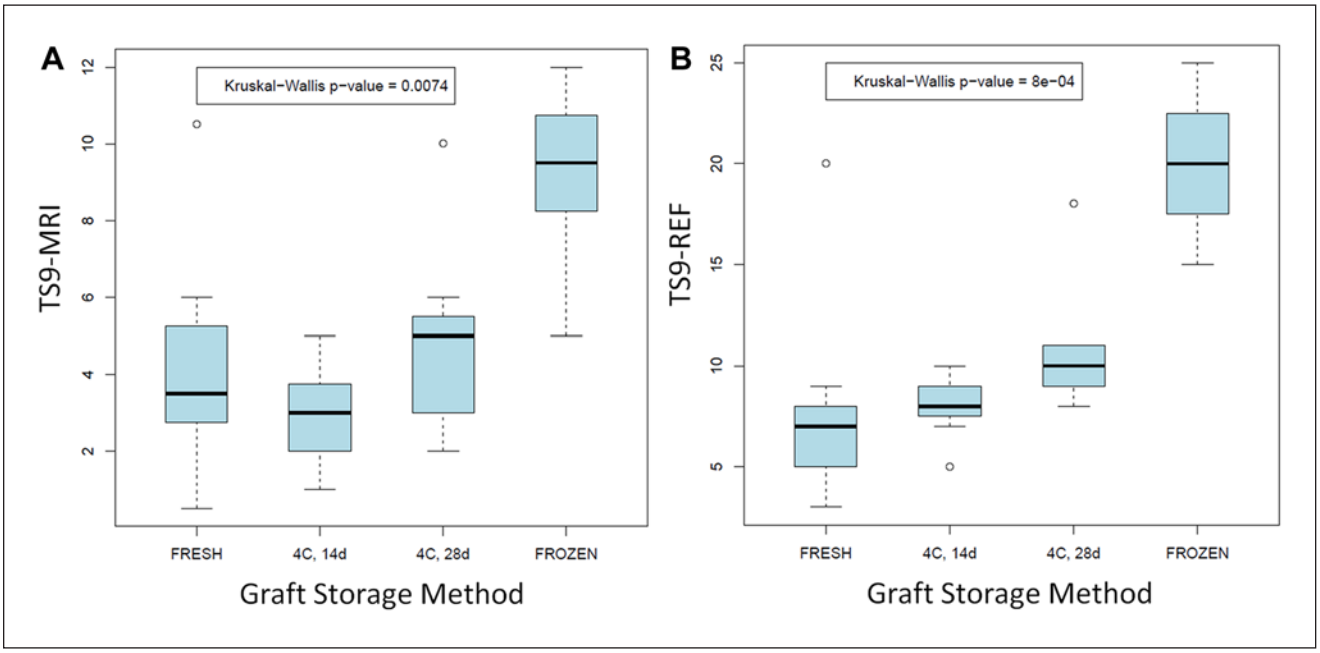

Figure 7. Boxplots of mean 9-feature MRI score (TS9-MRI) **(A)** and 9-feature reference standard score (TS9-REF) **(B)**. The Kruskal-Wallis test detected significant differences for TS9-MRI and TS9-REF with the frozen group performing worse than the other three groups (p = 0.007 and p = 0.001, respectively).

OCAMRISS with reference standard scores. Confidence intervals were reported to demonstrate the sample size-based estimate of the uncertainty around the correlation coefficient, its "projection onto reality". Regarding the correlation of TS9-MRI versus TS9-REF (Figure 5), the interpretation is that we are 95% confident that the true value is covered by the interval (the worst case of which is 0.708). Additionally, we attempted to simulate a spectrum of appearances by analyzing equal numbers of fresh, refrigerated (both 14 and 28 days), and frozen grafts. Despite this, we note that there was no variability in feature 8 (osseous integration), likely due to small sample size. We maintain that this is an important feature as we have noticed, as well as prior authors, that graft osseous nonunion can occur.[13,67] Second, caution must be exercised when applying these results to humans. Although we designed the scoring

Table 4. Comparison Between MOCART Score and Osteochondral Allograft Score.

MOCART Score	OCAMRISS
Feature 1: Degree of defect repair and filling of the defect	Feature 2: Cartilage "fill" of graft
Feature 2: Integration to border zone	Feature 3: Cartilage edge integration at host-graft junction
Feature 3: Surface of repair tissue	Feature 4: Cartilage surface congruity
Feature 4: Structure of repair tissue	Combination of feature 1 (cartilage signal of graft) and feature 2 (cartilage "fill" of graft)
Feature 5: Signal intensity of repair tissue	Feature 1: Cartilage signal of graft
Feature 6: Subchondral lamina	Feature 6: Subchondral bone plate congruity of graft and host-graft junction
Feature 7: Subchondral bone	Combination of feature 7 (subchondral bone marrow signal intensity of graft), feature 8 (osseous integration at host-graft junction), and feature 9 (presence of cystic changes of graft and host-graft junction)
Feature 8: Presence of adhesions	None
Feature 9: Presence of synovitis	Feature 12

MOCART, Magnetic Resonance Observation of Cartilage Repair Tissue; OCAMRISS, Osteochondral Allograft MRI Scoring System.

system based on our experience with human osteochondral allografts, due to the ethical challenges that would prohibit validation in humans, we chose to validate with an animal model. Of note, the goat is a large animal model that demonstrates a similar limited intrinsic healing potential of cartilage[68] and the 8-mm diameter grafts used in this study are larger than the critical size defect of 6 mm in goats.[69] Third, our semiquantitative classification system remains based on morphological MRI sequences. While some authors have found that conventional, qualitative MRI cannot predict histologic appearance (such as hyaline cartilage, fibrocartilage, or fibrous tissue),[70] additional studies should be performed evaluating quantitative MR biomarkers and their possible inclusion into classification systems. Fourth, although the UTE sequence was only used for evaluation of Feature 5 of OCAMRISS (integrity of the deep cartilage of the graft), there is potential for the UTE sequence to influence grading of other features. Fifth, higher imaging resolution was used in this study compared with a clinical human knee protocol in order to compensate for the smaller tissues in goats. Unfortunately, this led to the requirement of a lower receiver bandwidth in order to achieve adequate signal-to-noise ratio. Chemical shift was approximately 2.7 pixels on the proton density–weighted images. Although we did not feel that this adversely affected our interpretation, the degree of chemical shift is higher than that typically seen in clinical practice. Finally, we did not include clinical outcome measures and prior studies have suggested that certain MRI variables, such as trabecular incorporation, correlate with outcome measures.[22]

In conclusion, we described a comprehensive, semiquantitative MRI scoring system for the assessment of cartilage repair by osteochondral allografts, which we have termed OCAMRISS. We have demonstrated substantial interobserver agreement, substantial agreement with carefully selected reference standards for each component, and significant negative correlation with biomechanical indentation testing. The defined variables allow for an accurate description and may help standardize reporting of MR imaging findings after repair of cartilage defects with osteochondral allografts.

Acknowledgments and Funding

The authors thank Karen Bowden for technical histology assistance. This work was supported by the National Institutes of Health (grant numbers R01AR055637-02S1, R01DE022068). Eric Y. Chang receives salary support from a VA CSR&D Career Development Award (grant number 1IK2CX000749).

Declaration of Conflicting Interests

The author(s) declared no potential conflicts of interest with respect to the research, authorship, and/or publication of this article.

Ethical Approval

This study was approved by our institutional review board. All experiments were carried out in accordance with protocols approved by the Institutional Animal Care and Use Committee.

References

1. Curl WW, Krome J, Gordon ES, Rushing J, Smith BP, Poehling GG. Cartilage injuries: a review of 31,516 knee arthroscopies. Arthroscopy. 1997;13:456-60.
2. Robertsson O, Dunbar M, Pehrsson T, Knutson K, Lidgren L. Patient satisfaction after knee arthroplasty: a report on 27,372 knees operated on between 1981 and 1995 in Sweden. Acta Orthop Scand. 2000;71:262-7.
3. Hunziker EB. Articular cartilage repair: basic science and clinical progress. A review of the current status and prospects. Osteoarthritis Cartilage. 2002;10:432-63.
4. Delcogliano A, Caporaso A, Menghi A, Rinonapoli G, Chiossi S. Results of autologous osteochondral grafts in chondral lesions of the knee. Minerva Chir. 2002;57:273-81.
5. Jakob RP, Franz T, Gautier E, Mainil-Varlet P. Autologous osteochondral grafting in the knee: indication, results, and reflections. Clin Orthop Relat Res. 2002;(401):170-184.
6. LaPrade RF, Botker JC. Donor-site morbidity after osteochondral autograft transfer procedures. Arthroscopy. 2004;20:e69-73.

7. Vijayan S, Bartlett W, Bentley G, Carrington RW, Skinner JA, Pollock RC, *et al*. Autologous chondrocyte implantation for osteochondral lesions in the knee using a bilayer collagen membrane and bone graft: a two- to eight-year follow-up study. J Bone Joint Surg Br. 2012;94:488-92.
8. Filardo G, Vannini F, Marcacci M, Andriolo L, Ferruzzi A, Giannini S, *et al*. Matrix-assisted autologous chondrocyte transplantation for cartilage regeneration in osteoarthritic knees: results and failures at midterm follow-up. Am J Sports Med. 2013;41:95-100.
9. Langer F, Gross AE. Immunogenicity of allograft articular cartilage. J Bone Joint Surg Am. 1974;56:297-304.
10. Convery FR, Akeson WH, Meyers MH. The operative technique of fresh osteochondral allografting of the knee. Operat Tech Orthop. 1997;7:340-4.
11. Kalfas IH. Principles of bone healing. Neurosurg Focus. 2001;10:E1.
12. Prolo DJ, Rodrigo JJ. Contemporary bone graft physiology and surgery. Clin Orthop Relat Res. 1985;(200):322-42.
13. Brown D, Shirzad K, Lavigne SA, Crawford DC. Osseous integration after fresh osteochondral allograft transplantation to the distal femur: a prospective evaluation using computed tomography. Cartilage. 2011;2:337-45.
14. O'Driscoll SW, Keeley FW, Salter RB. The chondrogenic potential of free autogenous periosteal grafts for biological resurfacing of major full-thickness defects in joint surfaces under the influence of continuous passive motion. An experimental investigation in the rabbit. J Bone Joint Surg Am. 1986;68:1017-35.
15. Fleiss JL. The design and analysis of clinical experiments. New York: Wiley; 1986.
16. Peterson L, Minas T, Brittberg M, Nilsson A, Sjögren-Jansson E, Lindahl A. Two- to 9-year outcome after autologous chondrocyte transplantation of the knee. Clin Orthop Relat Res. 2000;(374):212-34.
17. Davidson PA, Rivenburgh DW, Dawson PE, Rozin R. Clinical, histologic, and radiographic outcomes of distal femoral resurfacing with hypothermically stored osteoarticular allografts. Am J Sports Med. 2007;35:1082-90.
18. Glenn RE Jr, McCarty EC, Potter HG, Juliao SF, Gordon JD, Spindler KP. Comparison of fresh osteochondral autografts and allografts: a canine model. Am J Sports Med. 2006;34:1084-93.
19. Henderson IJ, Tuy B, Connell D, Oakes B, Hettwer WH. Prospective clinical study of autologous chondrocyte implantation and correlation with MRI at three and 12 months. J Bone Joint Surg Br. 2003;85:1060-6.
20. Nemec SF, Marlovits S, Trattnig S. Persistent bone marrow edema after osteochondral autograft transplantation in the knee joint. Eur J Radiol. 2009;71:159-63.
21. Sirlin CB, Brossmann J, Boutin RD, Pathria MN, Convery FR, Bugbee W, *et al*. Shell osteochondral allografts of the knee: comparison of mr imaging findings and immunologic responses. Radiology. 2001;219:35-43.
22. Williams RJ 3rd, Ranawat AS, Potter HG, Carter T, Warren RF. Fresh stored allografts for the treatment of osteochondral defects of the knee. J Bone Joint Surg Am. 2007;89:718-26.
23. Orth P, Zurakowski D, Wincheringer D, Madry H. Reliability, reproducibility, and validation of five major histological scoring systems for experimental articular cartilage repair in the rabbit model. Tissue Eng Part C Methods. 2012;18:329-39.
24. Rutgers M, van Pelt MJ, Dhert WJ, Creemers LB, Saris DB. Evaluation of histological scoring systems for tissue-engineered, repaired and osteoarthritic cartilage. Osteoarthritis Cartilage. 2010;18:12-23.
25. Smith GD, Taylor J, Almqvist KF, Erggelet C, Knutsen G, Garcia Portabella M, *et al*. Arthroscopic assessment of cartilage repair: a validation study of 2 scoring systems. Arthroscopy. 2005;21:1462-7.
26. van den Borne MP, Raijmakers NJ, Vanlauwe J, Victor J, de Jong SN, Bellemans J, *et al*. International Cartilage Repair Society (ICRS) and Oswestry macroscopic cartilage evaluation scores validated for use in autologous chondrocyte implantation (ACI) and microfracture. Osteoarthritis Cartilage. 2007;15:1397-402.
27. de Windt TS, Welsch GH, Brittberg M, Vonk LA, Marlovits S, Trattnig S, *et al*. Is magnetic resonance imaging reliable in predicting clinical outcome after articular cartilage repair of the knee? A systematic review and meta-analysis. Am J Sports Med. 2013;41:1695-702.
28. Marlovits S, Striessnig G, Resinger CT, Aldrian SM, Vecsei V, Imhof H, *et al*. Definition of pertinent parameters for the evaluation of articular cartilage repair tissue with high-resolution magnetic resonance imaging. Eur J Radiol. 2004;52:310-9.
29. Welsch GH, Zak L, Mamisch TC, Resinger C, Marlovits S, Trattnig S. Three-dimensional magnetic resonance observation of cartilage repair tissue (MOCART) score assessed with an isotropic three-dimensional true fast imaging with steady-state precession sequence at 3.0 tesla. Invest Radiol. 2009;44:603-12.
30. Pallante AL, Chen AC, Ball ST, Amiel D, Masuda K, Sah RL, *et al*. The in vivo performance of osteochondral allografts in the goat is diminished with extended storage and decreased cartilage cellularity. Am J Sports Med. 2012;40:1814-23.
31. Du J, Bydder M, Takahashi AM, Carl M, Chung CB, Bydder GM. Short T2 contrast with three-dimensional ultrashort echo time imaging. Magn Reson Imaging. 2011;29:470-82.
32. Du J, Carl M, Bydder M, Takahashi A, Chung CB, Bydder GM. Qualitative and quantitative ultrashort echo time (UTE) imaging of cortical bone. J Magn Reson. 2010;207:304-11.
33. Eckstein F, Cicuttini F, Raynauld JP, Waterton JC, Peterfy C. Magnetic resonance imaging (MRI) of articular cartilage in knee osteoarthritis (OA): morphological assessment. Osteoarthritis Cartilage. 2006;14:A46-75.
34. De Smet AA. How i diagnose meniscal tears on knee MRI. AJR Am J Roentgenol. 2012;199:481-99.
35. De Smet AA, Tuite MJ. Use of the "two-slice-touch" rule for the MRI diagnosis of meniscal tears. AJR Am J Roentgenol. 2006;187:911-4.
36. Ogishima H, Tsuboi H, Umeda N, Horikoshi M, Kondo Y, Sugihara M, *et al*. Analysis of subclinical synovitis detected by ultrasonography and low-field magnetic resonance imaging in patients with rheumatoid arthritis. Mod Rheumatol. Epub 2013 Mar 3.
37. Hill CL, Hunter DJ, Niu J, Clancy M, Guermazi A, Genant H, *et al*. Synovitis detected on magnetic resonance imaging and its relation to pain and cartilage loss in knee osteoarthritis. Ann Rheum Dis. 2007;66:1599-603.
38. Roemer FW, Guermazi A, Zhang YQ, Yang M, Hunter DJ, Crema MD, *et al*. Hoffa's fat pad: evaluation on unenhanced

MR images as a measure of patellofemoral synovitis in osteoarthritis. AJR Am J Roentgenol. 2009;192:1696-700.
39. Shapiro F, Glimcher MJ. Induction of osteoarthrosis in the rabbit knee joint. Clin Orthop Relat Res. 1980;(147):287-95.
40. Bergman AG, Willen HK, Lindstrand AL, Pettersson HT. Osteoarthritis of the knee: correlation of subchondral MR signal abnormalities with histopathologic and radiographic features. Skeletal Radiol. 1994;23:445-8.
41. Zanetti M, Bruder E, Romero J, Hodler J. Bone marrow edema pattern in osteoarthritic knees: correlation between MR imaging and histologic findings. Radiology. 2000;215:835-40.
42. Landis JR, Koch GG. The measurement of observer agreement for categorical data. Biometrics. 1977;33:159-74.
43. LaPrade RF, Botker J, Herzog M, Agel J. Refrigerated osteoarticular allografts to treat articular cartilage defects of the femoral condyles. A prospective outcomes study. J Bone Joint Surg Am. 2009;91:805-11.
44. McDermott AG, Langer F, Pritzker KP, Gross AE. Fresh small-fragment osteochondral allografts. Long-term follow-up study on first 100 cases. Clin Orthop Relat Res. 1985;(197):96-102.
45. Meyers MH, Akeson W, Convery FR. Resurfacing of the knee with fresh osteochondral allograft. J Bone Joint Surg Am. 1989;71:704-13.
46. Pallante AL, Gortz S, Chen AC, Healey RM, Chase DC, Ball ST, *et al*. Treatment of articular cartilage defects in the goat with frozen versus fresh osteochondral allografts: effects on cartilage stiffness, zonal composition, and structure at six months. J Bone Joint Surg Am. 2012;94:1984-95.
47. Goebel L, Orth P, Muller A, Zurakowski D, Bucker A, Cucchiarini M, *et al*. Experimental scoring systems for macroscopic articular cartilage repair correlate with the MOCART score assessed by a high-field MRI at 9.4 T—comparative evaluation of five macroscopic scoring systems in a large animal cartilage defect model. Osteoarthritis Cartilage. 2012;20:1046-55.
48. Lee KT, Choi YS, Lee YK, Cha SD, Koo HM. Comparison of MRI and arthroscopy in modified MOCART scoring system after autologous chondrocyte implantation for osteochondral lesion of the talus. Orthopedics. 2011;34:e356-62.
49. Tetta C, Busacca M, Moio A, Rinaldi R, Delcogliano M, Kon E, *et al*. Knee osteochondral autologous transplantation: long-term MR findings and clinical correlations. Eur J Radiol. 2010;76:117-23.
50. Link TM, Mischung J, Wortler K, Burkart A, Rummeny EJ, Imhoff AB. Normal and pathological MR findings in osteochondral autografts with longitudinal follow-up. Eur Radiol. 2006;16:88-96.
51. Trattnig S, Millington SA, Szomolanyi P, Marlovits S. MR imaging of osteochondral grafts and autologous chondrocyte implantation. Eur Radiol. 2007;17:103-18.
52. Lane JG, Tontz WL Jr, Ball ST, Massie JB, Chen AC, Bae WC, *et al*. A morphologic, biochemical, and biomechanical assessment of short-term effects of osteochondral autograft plug transfer in an animal model. Arthroscopy. 2001;17:856-63.
53. Oates KM, Chen AC, Young EP, Kwan MK, Amiel D, Convery FR. Effect of tissue culture storage on the in vivo survival of canine osteochondral allografts. J Orthop Res. 1995;13:562-9.
54. Schachar NS, Novak K, Hurtig M, Muldrew K, McPherson R, Wohl G, *et al*. Transplantation of cryopreserved osteochondral Dowel allografts for repair of focal articular defects in an ovine model. J Orthop Res. 1999;17:909-19.
55. Roberts S, McCall IW, Darby AJ, Menage J, Evans H, Harrison PE, *et al*. Autologous chondrocyte implantation for cartilage repair: monitoring its success by magnetic resonance imaging and histology. Arthritis Res Ther. 2003;5:R60-73.
56. Bae WC, Dwek JR, Znamirowski R, Statum SM, Hermida JC, D'Lima DD, *et al*. Ultrashort echo time MR imaging of osteochondral junction of the knee at 3 T: identification of anatomic structures contributing to signal intensity. Radiology. 2010;254:837-45.
57. Bae WC, Statum S, Zhang Z, Yamaguchi T, Wolfson T, Gamst AC, *et al*. Morphology of the cartilaginous endplates in human intervertebral disks with ultrashort echo time MR imaging. Radiology. 2013;266:564-74.
58. Green WT Jr, Martin GN, Eanes ED, Sokoloff L. Microradiographic study of the calcified layer of articular cartilage. Arch Pathol. 1970;90:151-8.
59. Burr DB. Anatomy and physiology of the mineralized tissues: role in the pathogenesis of osteoarthrosis. Osteoarthritis Cartilage. 2004;12(Suppl A):S20-30.
60. Hwang J, Bae WC, Shieu W, Lewis CW, Bugbee WD, Sah RL. Increased hydraulic conductance of human articular cartilage and subchondral bone plate with progression of osteoarthritis. Arthritis Rheum. 2008;58:3831-42.
61. Oettmeier R, Arokoski J, Roth AJ, Helminen HJ, Tammi M, Abendroth K. Quantitative study of articular cartilage and subchondral bone remodeling in the knee joint of dogs after strenuous running training. J Bone Miner Res. 1992;7(Suppl 2):S419-24.
62. Mow VC, Bachrach NM, Ateshian GA. The effects of a subchondral bone perforation on the load support mechanism within articular-cartilage. Wear. 1994;175:167-75.
63. Beaver RJ, Mahomed M, Backstein D, Davis A, Zukor DJ, Gross AE. Fresh osteochondral allografts for post-traumatic defects in the knee. A survivorship analysis. J Bone Joint Surg Br. 1992;74:105-10.
64. Chu CR, Convery FR, Akeson WH, Meyers M, Amiel D. Articular cartilage transplantation. Clinical results in the knee. Clin Orthop Relat Res 1999;(360):159-68.
65. Jamali AA, Emmerson BC, Chung C, Convery FR, Bugbee WD. Fresh osteochondral allografts: results in the patellofemoral joint. Clin Orthop Relat Res 2005;(437):176-85.
66. Torga Spak R, Teitge RA. Fresh osteochondral allografts for patellofemoral arthritis: long-term followup. Clin Orthop Relat Res. 2006;(444):193-200.
67. Gross AE, Shasha N, Aubin P. Long-term followup of the use of fresh osteochondral allografts for posttraumatic knee defects. Clin Orthop Relat Res 2005;(435):79-87.
68. Chu CR, Szczodry M, Bruno S. Animal models for cartilage regeneration and repair. Tissue Eng Part B Rev 2010;16:105-15.
69. Jackson DW, Lalor PA, Aberman HM, Simon TM. Spontaneous repair of full-thickness defects of articular cartilage in a goat model. A preliminary study. J Bone Joint Surg Am. 2001;83:53-64.
70. Tins BJ, McCall IW, Takahashi T, Cassar-Pullicino V, Roberts S, Ashton B, *et al*. Autologous chondrocyte implantation in knee joint: MR imaging and histologic features at 1-year follow-up. Radiology. 2005;234:501-8.